XV International Conference on Durability of Building Materials and Components
DBMC 2020, Barcelona
C. Serrat, J.R. Casas and V. Gibert (Eds)

On the Effects of Relative Humidity and CO_2 Concentration on Carbonation of Cement Pastes

Quoc Tri Phung[1], Anna Varzina[1,2], Janez Perko[1], Diederik Jacques[1], Norbert Maes[1] and Özlem Cizer[2]

[1]Waste & Disposal, Belgian Nuclear Research Centre (SCK CEN), Boeretang 200, 2400 Mol, Belgium, {qphung, avarzina, jperko, djacques, nmaes}@sckcen.be

[2]Building Materials and Building Technology Section, KU Leuven, 3001 Leuven, Belgium, ozlem.cizer@kuleuven.be

Abstract. *Many environments to which concrete is exposed are highly aggressive due to various chemical components. In such environments, concrete is subjected to processes of chemical degradation, among which carbonation is one of the most frequently seen degradation processes. Though, the influence of saturation degree (or relative humidity - RH) of the specimen and CO_2 concentration on the carbonation of cementitious materials is still not comprehensively described with respect to carbonation rate/degree as well as alteration in microstructure and mineralogy. This work aims at thoroughly investigating how these two key parameters affect the carbonation under accelerated conditions. Furthermore, the effect of initial moisture state of the specimen on the carbonation rate is also demonstrated. For such purpose, a numerical model at continuum scale is developed to investigate the effects of RH and CO_2 concentration on the carbonation depth, phase changes in phases and porosity of hardened cement pastes due to carbonation under accelerated conditions. Verification with experimental results from accelerated carbonation tests shows a good agreement. The modelling results with supporting experimental data help to better understand the modification of material properties under different carbonation conditions and to optimize the carbonation conditions.*

Keywords: *Carbonation, CO_2 Concentration, Microstructure, Cement Paste, Relative Humidity.*

1 Introduction

The carbonation process in cement-based materials is typically considered as a deterioration phenomenon because it results in a pH decrease, which accelerates the corrosion of reinforcing bars in concrete. On the other hand, carbonation also results in beneficial effects including decreases in transport properties and refines the pore structure of cement-based materials (Phung *et al.*, 2015; Phung *et al.*, 2016b). The extent of modification in transport properties and microstructure significantly depends on carbonation conditions (*e.g.* CO_2 concentration, relative humidity) and cement types (*e.g.* OPC or blended systems). The reduction of transport properties is the result of the precipitation of carbonation products in the pore structure, which leads to a significant reduction of the total porosity (Phung, 2015).

A number of models have been proposed based on Fick's law for diffusion with an analytical relation between the carbonation depth and square root of time. Instead of giving an explicit formula to predict the carbonation depth, a large number of models have been developed in order to solve the carbonation problem numerically (Bary *et al.*, 2004; Muntean *et al.*, 2011). These approaches are based on conservation laws with a complex form to capture the most important factors (including other transport rather than diffusion and time-dependent variables, *e.g.* porosity) influencing the carbonation process. However, identification of parameters for complex models may require several experiments and is not an easy task, for example to parameterize a constitutive relation between relative humidity, porosity changes and diffusivity

of CO_2 during carbonation. In a previous study (Phung *et al.*, 2016a), the authors have successfully developed a comprehensive 1-D reactive transport model accounting for both advective and diffusive transports under an applied CO_2 pressure gradients. The model enables to predict carbonation depth and changes in permeability, diffusivity, and porosity due to carbonation. In this study, a reduced form of the previous model with only diffusive transport is used in order to investigate the key parameters (*e.g.* RH, CO_2 concentration, w/c ratios), which are applied in conventional accelerated carbonation experiments. In such a common way, the samples are put in a controlled chamber at a wide range of CO_2 concentrations (*e.g.* 0.1% to 10%) and an optimized relative humidity (50-70%) to speed up carbonation. Results from such accelerated carbonation data are scattered and sometimes contrary due to wide ranges of carbonation conditions. Moreover, the moisture content of the tested samples is not always similar or even different from the surrounding environment in accelerated carbonation chamber. This leads to a big uncertainty despite of the same carbonation conditions. The above issues are intensively discussed in this work by numerical simulation in combination with preliminary validation with experimental data.

2 Model Development

The proposed model is based on a macroscopic mass balance for CO_2 in gaseous and aqueous phases. The model only considers the carbonation of portlandite and C-S-H, which are the main hydrated phases in CEM I ordinary Portland cement (OPC) paste. Continuous hydration of the samples during carbonation is not taken into account as the experiments were conducted on 28-day-old samples and the time for carbonation was quite limited.

2.1 Mass Conservation of CO_2

2.1.1 Transport of CO_2

The total concentration of CO_2 in the porous media is the sum of the amounts of CO_2 in the gaseous and aqueous phases:

$$c = \phi(1-S)c_g + \phi S c_l \tag{1}$$

where ϕ is porosity; S is water saturation degree; c_g and c_l are the concentrations of gaseous and dissolved carbon dioxide, respectively, which can be related by using Henry law and Clapeyron equation,

$$c_g = c_l K_H / RT \tag{2}$$

where and K_H denotes the Henry constant; R is universal gas constant; T is absolute temperature. The total flux of CO_2 includes both the CO_2 fluxes in the gaseous and aqueous phase, expressed as:

$$J = D_g \frac{\partial c_g}{\partial x} + D_l \frac{\partial c_l}{\partial x} = \left(\frac{K_H}{RT} D_g + D_l \right) \frac{\partial c_l}{\partial x} \tag{3}$$

where D_g and D_l are effective diffusion coefficients of gaseous and aqueous phase, respectively. In porous media, the effective diffusion coefficient depends on the pore structure (Phung *et al.*, 2019a). For the effective diffusion coefficient D_l of dissolved CO_2, we account for the changes in porosity, tortuosity, carbonation degree ($k_{Dl}^*(\phi,\tau)$) and saturation degree ($k_{Dl}(S)$) during carbonation followed as (Phung *et al.*, 2016a):

$$D_l = D_{l0} \times k_{Dl}^*(\phi,\tau) \times k_{Dl}(S) \tag{4}$$

For CO_2 diffusion in the gaseous phase, a similar approach as in the aqueous phase is adopted. However, Knudsen diffusion is taken into account through the factor k_{Knu} because carbonation shifts the pore size distribution towards smaller pores (Phung *et al.*, 2015) which results in a smaller effective diffusivity for carbonated material.

$$D_g = D_{g0} \times k_{Dg}^{*}(\phi,\tau) \times k_{Dg}(S) \times k_{Knu} \tag{5}$$

Details of these models for the diffusivity can be found in (Phung *et al.*, 2016a).

2.1.2 Evolution of porosity during carbonation

The change in porosity is obtained from the change in solid phases by carbonation of portlandite and C-S-H.

$Ca(OH)_2 + CO_2 = CaCO_3 + H_2O$

$$\Delta\phi_{CH} = \left[\left(C_{CH0} - C_{CH}\right)/M_{CH}\right]\left(V_{CH} - V_{CC}\right) \tag{6}$$

$y_0CaO{\bullet}SiO_2{\bullet}z_0H_2O + (y_0\text{-}y)CO_2 = yCaO{\bullet}SiO_2{\bullet}zH_2O + (y_0\text{-}y)CaCO_3 + (z_0\text{-}z)H_2O$

$$\Delta\phi_{CSH} = C_{CSH0}/M_{CSH0}\left[\left(y_0 - y\right)V_{CC} - \left(V_{CSH0} - V_{CSH}\right)\right] \tag{7}$$

where $\Delta\phi_{CH}$ and $\Delta\phi_{CSH}$ are porosity changes [-] due to portlandite and C-S-H carbonation, respectively; y and z are the average Ca/Si ratio and stoichiometric ratio of H_2O in C-S-H, respectively; C_{CH} and C_{CSH} are portlandite and C-S-H contents, respectively; M_{CH} and M_{CSH0} are molar masses of portlandite and C-S-H, respectively; V_{CH}, V_{CC} and V_{CSH} are molar volumes of portlandite, calcite and C-S-H, respectively. Subscript 0 denotes the initial condition. The molar volumes of portlandite and calcite are well defined in literature. However, data for molar volume of C-S-H are scarce and it is a stoichiometry-dependent parameter. An experimental study (Morandeau *et al.*, 2014) showed that the molar volume of C-S-H is proportional to the Ca/Si ratio as:

$$V_{CSH0} - V_{CSH} = \omega\left(1 - y/y_0\right) \tag{8}$$

where $0.02 < \omega < 0.04$ [l/mol]. The total porosity of sample during carbonation is expressed as follows:

$$\phi = \phi_0 + \Delta\phi_{CH} + \Delta\phi_{CSH} \tag{9}$$

where ϕ_0 is initial total porosity. The change in capillary porosity is mainly due to the carbonation of portlandite as majority of portlandite particles are located near the capillary pores (Phung *et al.*, 2015). However, C-S-H carbonation might partially contribute to the capillary porosity change, especially under accelerated conditions. The partial contribution of C-S-H carbonation to capillary porosity is captured by a coefficient υ ($0 \le \upsilon \le 1$) as:

$$\phi_c = \phi_{c0} + \Delta\phi_{CH} + \upsilon\Delta\phi_{CSH} \tag{10}$$

where ϕ_{c0} is initial capillary porosity. The value of υ is set to be 0.5 for OPC cement paste which gives a good fit with capillary porosity change determined by MIP (Phung *et al.*, 2016a).

2.1.3 Carbonation reaction

Instead of separately modelling the carbonation reactions of CH and C-S-H, we combine both reactions as in a single reaction between Ca^{2+} (dissolved from CH and C-S-H) and CO_3^{2-} ions:

$$Ca^{2+}{}_{(total)} + CO_3^{2-} \rightarrow CaCO_3 \tag{11}$$

We consider that the reaction (11) is of the first order with respect to Ca^{2+} and CO_3^{2-} concentration. The rate of the combined carbonation reaction, r, is written as:

$$r = k_C f(S) k_r \frac{C_{Ca}}{M_{Ca}} \frac{C_{CO_3}}{M_{CO_3}} \tag{12}$$

where k_C is the temperature-dependent reaction rate coefficient, M_{Ca} and M_{CO3} are molar masses of Ca^{2+} and CO_3^{2-}, respectively. The factor *f(S)* corrects the kinetic carbonation reaction rate coefficient for the effect of water saturation degree. Following the approach of (Papadakis *et al.*, 1991),

$$f(S) = S^n \tag{13}$$

where the parameter *n* is suggested to be 3.7. The carbonation products are mainly formed around CH/C-S-H particles. Consequently, the reaction rate will reduce because Ca ion and CO_2 have to diffuse through the product layer. Therefore, a retardation factor is added into Eq. (12) as:

$$k_r = \left(C_{Ca}^s / C_{Ca0}^s \right)^{\Theta} \tag{14}$$

where C_{Ca}^s is total concentration of solid Ca except for Ca in calcium carbonate, subscript 0 denotes the initial concentration; Θ is exponential factor which is suggested to be 2 for OPC cement paste (Phung *et al.*, 2016a).

The mass balance of dissolved CO_2 is written as:

$$\frac{\partial \left(\left[\phi(1-S) \frac{K_{CO_2}^H}{RT} + \phi S \right] c_l \right)}{\partial t} - \frac{\partial \left(\left[\frac{K_{CO_2}^H}{RT} D_g + D_l \right] \frac{\partial c_l}{\partial x} \right)}{\partial x} = -f(S) \phi k_C k_r \frac{C_{Ca}}{M_{Ca}} \frac{C_{CO_3}}{M_{CO_3}} M_{CO_2} \tag{15}$$

The partial differential Eq. (15) describes the one-dimensional reaction-transport phenomenon in cement-based materials and is solved numerically using the COMSOL Multiphysics® FEM based simulation tool.

2.2 Mass Conservation of Calcium

Following the same approach for CO_2, the mass balance equation for total dissolved Ca is given as:

$$\frac{\partial \left(\phi S C_{Ca} \right)}{\partial t} - \frac{\partial \left(D_{Ca} \frac{\partial C_{Ca}}{\partial x} \right)}{\partial x} = -\phi r \frac{M_{Ca}}{M_{CO_2}} + r_d \tag{16}$$

where D_{Ca} is the effective diffusivity of calcium ion; r_d is the dissolution rate of CH and C-S-H [kg/m^3.s] which is calculated from the mass balance equation of total amount of Ca in CH and C-S-H as follows:

$$\frac{\partial C_{Ca}^s}{\partial t} M_{Ca} = -r_d \tag{17}$$

Note that in Eq. (17) the release rate of Ca due to hydration is neglected. The solid-liquid equilibrium curve of Ca based on the experimental data collected by (Berner, 1992) is used to establish a relation between the aqueous and solid calcium concentration which is expressed as an mathematical form based on a discretization of the decalcification of CH and C–S–H (Phung *et al.*, 2016a). The Ca fraction in CH and C-S-H can be estimated from the hydration of minerals (C_2S, C_3S) in cement which can be estimated by the Bouge calculation.

2.3 Mass Conservation of Moisture

2.3.1 Liquid water transport

The mass balance equation for liquid water (excluding bound water) is given as:

$$\frac{\partial(\phi S\gamma_l)}{\partial t} = -\mu_E - \mu_R \tag{18}$$

where μ_E is the vapour-liquid water exchange rate; and μ_R is the released water rate due to carbonation. The amount of water released is derived from the carbonation reactions Eqs. (6) and (7), for CH and C-S-H, respectively. For CH, there is a 1-1 relation between Ca consumption and water release. However, for C-S-H carbonation, y mol of Ca in C-S-H will release z mol H_2O. The stoichiometry values of y and z are only slightly different (Allen *et al.*, 2007). Therefore, we assume that ratio $y/z = 1$. With this assumption, it is possible to calculate the amount of released water rate based on the change of total Ca in solid phase.

$$\mu_R = \frac{\partial\left(\left(C_{Ca}^{s} - C_{Ca}^{s0}\right)M_w\right)}{\partial t} \tag{19}$$

where M_w is molar weight of water, C_{Ca}^{s0} is initial Ca content in the solid phases.

2.3.2 Vapour transport

Vapour is transported due to diffusion. The mass balance equation for vapour is given as:

$$\frac{\partial(\phi c_v(1-S))}{\partial t} + \frac{\partial\left(\phi(1-S)D_v\frac{\partial c_v}{\partial x}\right)}{\partial x} = \mu_E \tag{20}$$

where c_v is the concentration of vapour which is calculated as

$$c_v = P_v M_w / RT \tag{21}$$

where P_v is the partial pressure of vapour which is depended on relative humidity,

$$P_v = RH \times P_{vs} \tag{22}$$

where P_{vs} is the average saturation pressure of vapour; D_v is the diffusivity of vapour.

3 Description of Carbonation Experiments

Accelerated carbonation experiments were performed on cement pastes at three w/c ratios of 0.4, 0.5 and 0.6. Type I ordinary Portland cement (CEM I 52.5 N) was used. The chemical and physical properties of the cement can be found in (Phung *et al.*, 2019b). Cement pastes were cast in a cylindrical tube with an inner diameter of 98 mm and cured in sealed conditions. After 28 days of curing, the samples were cut into small disks of 25 mm thick by a diamond saw. Prior to the carbonation experiment, the samples were conditioned to different target internal relative humidity of 55%, 65% and 75% in a climate chamber. Note that sample conditioning is an essential step that would significantly affect the carbonation results as shown later in section 4.4. In our case the samples is ensure to reach the targeted RH when the mass of sample is stable. The accelerated carbonation tests were performed in 28 days at constant temperature of 20°C. Two CO_2 concentrations of 0.3% and 1% and three RH of 55%, 65% and 75% were investigated. Details of the setup and experimental procedure were described in (Varzina *et al.*, In preparation).

After carbonation, a number of post-analysis methods were used to quantitatively and qualitatively analyse the carbonated samples. The carbonated sample was sawn and sprayed by phenolphthalein solution to determine the phenolphthalein carbonation depth (Phung *et al.*, 2015). Portlandite and calcium carbonate profiles of a carbonated sample were quantified by thermo-gravimetric analysis (TGA) of the dust collected at different depths. A hole with a diameter of 10 mm was longitudinally drilled in the carbonated sample. Drilling was halted

every 3 mm to collect the dust before continuing drilling. To prevent cross contamination, the hole was carefully cleaned by compressed air before continuing drilling. TGA was performed in a NETZSCH STA 449F3 thermal analyzer. A weighed sample, usually between 30 and 40 mg was heated from room temperature to 1100°C with a heating rate of 10°C per minute under a constant nitrogen flow rate of 120 ml/min.

Mercury intrusion porosimetry (MIP) provided information on how pore structure changes during carbonation. MIP experiments were performed in a PASCAL 140/440 porosimeter in which the mercury pressure was continuously increased up to a maximum pressure of 200 MPa. The samples were taken from the reactive surface up to 3 mm in depth and referred as "carbonated samples". Furthermore, the mass of samples were followed as a function of carbonation time, which allows calculating the mass gain due to carbonation.

4 Results and Validation

4.1 Carbonation Degree

The term "carbonation depth" is typically determined by a phenolphthalein indicator. However, it is not easy to mathematically define the carbonation depth. In this study, we relate the carbonation depth to total concentration of Ca in the solid phases (C_{Ca}^{s}). In such way, carbonation depth is linked to a maximum depth at which portlandite (CH) is completely carbonated, and referred as carbonation degree of 1. The carbonation degree, d_c, is then formulated as:

$$d_c = \begin{cases} 1 & CH < 0 \\ \dfrac{C_{Ca}^{s0} - C_{Ca}^{s}}{C_{Ca}^{CH}} & CH \geq 0 \end{cases} \tag{23}$$

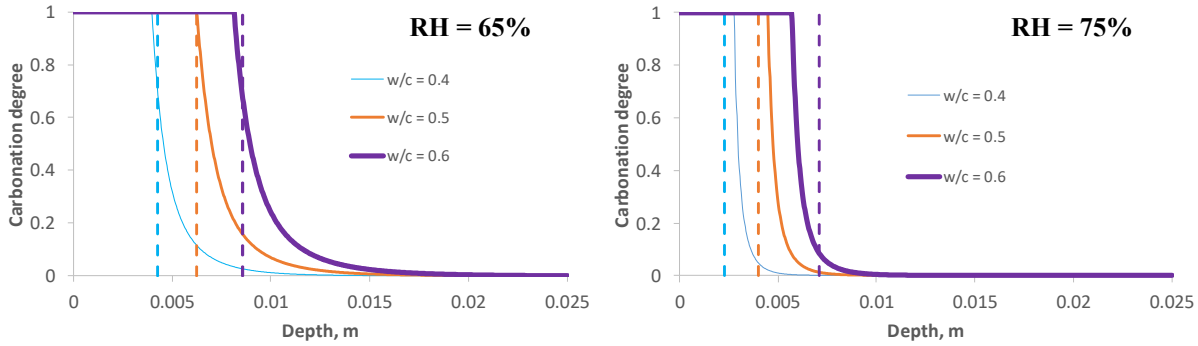

Figure 1. Carbonation degree of samples carbonated at RH of 65% and 75%, CO_2 concentration of 1% - dashed lines mark the carbonation depths determined by phenolphthalein spraying.

The carbonation degree of samples with different w/c ratios carbonated with CO_2 concentration of 1% at RH at 65% and 75% is shown in Figure 1. It is clearly seen that the higher w/c ratios, the larger carbonation degree. A higher RH results in a lower carbonation degree. Interestingly, the transition zone (*i.e.* d_c<1) is wider for carbonation at lower RH, meaning a sharp carbonation front might not be observed in this case. This is explained by a faster diffusion of CO_2 under lower RH condition. Comparing with carbonation depth determined by phenolphthalein indicator, the carbonation degree agrees very well with the phenolphthalein front (i.e. the front is corresponded to carbonation degree of 1) for 65% RH. Results at higher RH is in less agreement, especially for the sample with w/c ratio of 0.6.

4.2 Mass Gain

In this study, the sample mass gain is considered as the sum of CO_2 uptake and change in moisture content of carbonated sample. We can easily calculate the total CO_2 uptake due to the carbonation reactions of portlandite and C-S-H. Considering Eq. (11), the number of moles of solid Ca consumed equals the number of moles of CO_2 uptake. The moisture content change is related to the differences in saturation degree (mass change due to different RH is negligible). Therefore, the mass gain (normalized to initial sample mass) due to carbonation can be expressed as:

$$Mass = 100\% \int_0^L \left\{ \left[\left(C_{Ca}^{s0} - C_{Ca}^{s} \right) + \left(C_{Ca}^{0}\phi_0 - C_{Ca}\phi \right) \right] M_{CO_2} + \left(S\phi - S_0\phi_0 \right) \rho_w \right\} A / m_{sam} dx \qquad (24)$$

where A and m_{sam} are the cross section and initial mass of the sample, respectively.

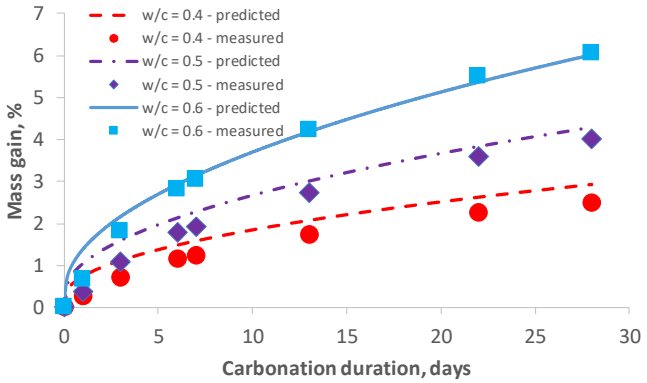

Figure 2. Mass gain of samples carbonated at RH of 65% and CO_2 concentration of 1%.

As expected, higher w/c ratio results in higher mass gain as seen in Figure 2. The predicted results agree very well with the measured data. Note that the mass gain is not equal to the CO_2 uptake because of the moisture content exchange of the samples with surrounding environment during carbonation, which is well captured in the model.

4.3 Effect of Carbonation Conditions

4.3.1 Relative humidity

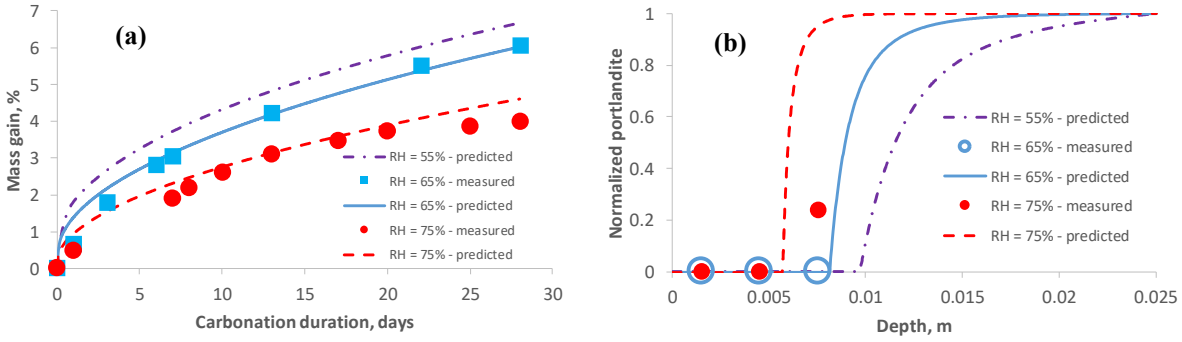

Figure 3. Effects of RH on mass gain (a) and change in portlandite content after 28 days of carbonation (b) – measured data for RH = 55% is not yet available.

Typically, a wide range of RH is used in accelerated carbonation experiments. The European standard EN 12395 even allows the tests performing with RH = 60%±10%. We therefore simulate the carbonation under various RH of 55%, 65% and 75%. Results show that the carbonation rate is significantly depended on the RH of the surrounding environment. The lower

RH, the higher mass gain and percentage of carbonated portlandite (Figure 3). The mass gain is increased 30% if RH decreases from 75% to 55%. Similarly, the depth of complete portlandite carbonation increases from 6 mm to 10 mm with a decrease of RH from 75% to 55%.

As a consequence, the drop in capillary porosity due to carbonation is more visible for lower RH as shown in Figure 4. The effects of RH is much clearer in case of higher w/c ratio.

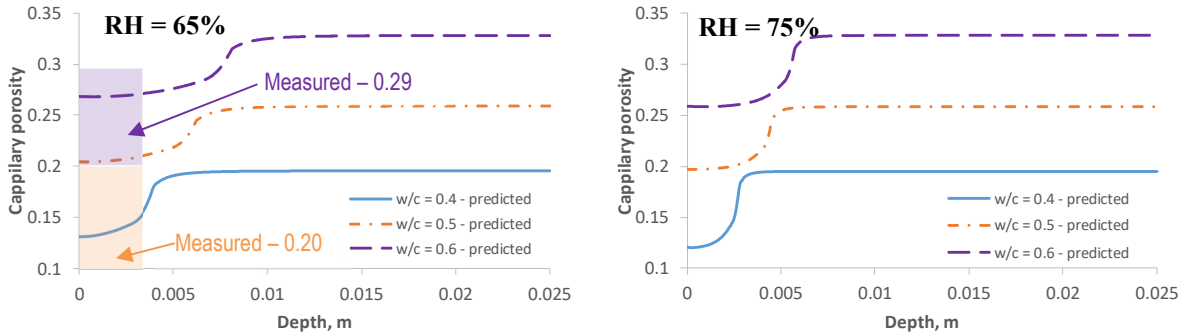

Figure 4. Effects of RH on capillary porosity decrease due to carbonation at 1% CO_2 concentration.

4.3.2 CO_2 concentration

The CO_2 concentration significantly influences the carbonation in terms of mass gain. Increasing CO_2 concentration from 0.3% to 3% triples the mass gain as seen in Figure 5a. This is a consequence of a higher amount of portlandite carbonation as shown in Figure 5b. The C/S ratio of C-S-H is also significantly reduced in the portlandite depletion zone, which is in agreement with thermodynamic modelling results showing that initially no C-S-H should decalcify. However, this sometimes does not comply with experimental findings, e.g. (Auroy *et al.*, 2018; Phung *et al.*, 2015) which showed evidences that carbonation of portlandite and other hydrated phases may occur simultaneously. In case of highest CO_2 concentration, the C/S ratio can be lower than 0.4 near the reactive surface. Interestingly, C-S-H is carbonated with the highest extent not at the reactive surface, but around 3 mm far away the reactive surface indicating that the optimal carbonation conditions (*i.e.* reaction rate, available CO_2 and Ca) occur a bit far away from the reactive surface if higher CO_2 concentration is applied.

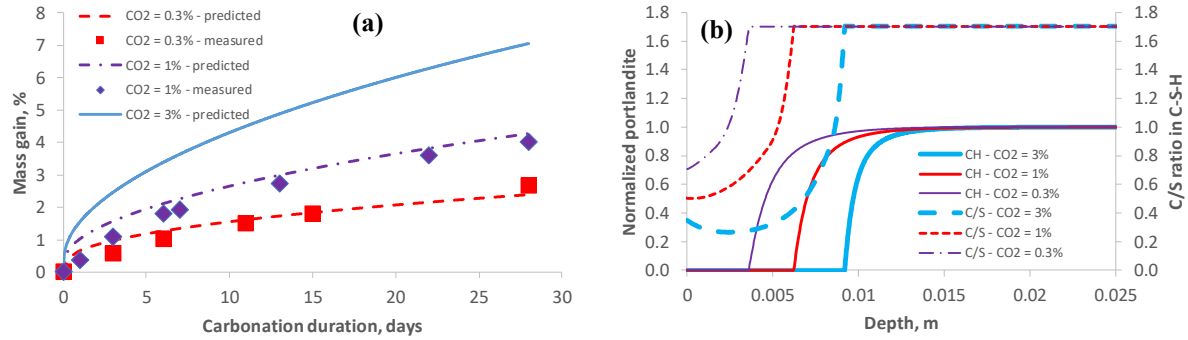

Figure 5. Effects of CO_2 concentration on mass gain (a) and changes in portlandite content and C/S ratio of C-S-H after 28 day carbonation (b) - samples with the same w/c ratio of 0.5 and carbonated under 65% RH, measured mass gain for case CO_2 = 3% is not yet available.

4.4 Effect of Sample Preparation – Initial Relative Humidity

In practice, the samples are not always well-conditioned to reach the targeted RH humidity in the carbonation chamber. The conditioning process could take few weeks to months (depended on sample size and w/c ratio) to bring the initial moisture state (RH>95%) to the optimal

carbonation RH of around 65%. If the initial RH of samples differs from the RH of carbonation chamber, the results can be significantly scattered. Figure 6 illustrates such uncertainty by investigating 3 initial RH levels of 65%, 80% and 85%. All samples with w/c ratio of 0.5 are carbonated under the same conditions with RH of 65% and CO_2 concentration of 1% at 20°C. It is clearly seen that higher initial RHs significantly reduce the carbonation degree. This is because the internal RH and saturation of these samples are much higher than the one with initial RH of 65% (Figure 6b), resulting in much slower transport of CO_2 into the samples. It is interesting to observe that a maximum RH is obtained at the depth where carbonation degree starts decreasing. This is explained by the accumulation of water released by carbonation, which does not have enough time to transport to the surrounding environment. The slower transport of CO_2 in samples with higher initial RH also induces higher C-S-H carbonation resulting in lower C/S ratio as seen in Figure 6a.

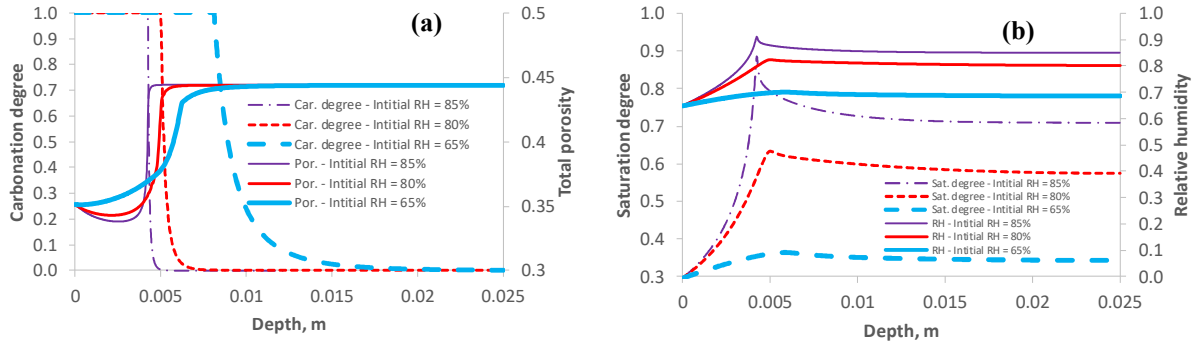

Figure 6. Effects of initial RH of samples on carbonation degree and total porosity alteration (a) and saturation degree and internal RH of carbonated samples (b).

5 Conclusions

A one-dimensional reactive transport model coupling moisture – CO_2 – Ca transport, which is adapted from a previous work (Phung *et al.*, 2016a), is implemented to investigate the effects of RH and CO_2 concentration and initial moisture state of the samples on the carbonation degree, phase changes and porosity of hardened cement pastes due to carbonation under accelerated conditions. The model enables to predict the carbonation degree, mass gain, portlandite content, C/S ratio and porosity change over time and space. A parametric study confirms that two key parameters, i.e. CO_2 concentration and RH, play an important role in accelerated carbonation of cement pastes. Variation of these parameters in a common testing range could significantly change the carbonation degree; however, their effects also depend on the microstructure of the samples which is controlled by the w/c ratios. The higher the w/c ratios, the larger the contribution of RH and CO_2 concentration. The model helps to better interpret the experimental observations and highlights underlying phenomena such as the formation of a gradual carbonation front due to carbonation of both portlandite and C-S-H or changes in moisture state along the sample depth. Furthermore, the modelling results confirm the vital contribution of initial moisture state of the samples to the carbonation process and estimated carbonation rate. Poor sample conditioning (i.e. too short time to lower the initial RH after curing to targeted testing RH) could dramatically reduce the carbonation efficiency.

Preliminary verification of the modelling results with accelerated carbonation experiment gives a good agreement even though more experimental data is still required to validate and improve the model, especially to better capture changes in transport properties due to carbonation.

Acknowledgements

This work is financially supported from ENGIE via the project 068 'CARBOCRACK'.

ORCID

Quoc Tri Phung: https://orcid.org/0000-0001-9859-860X

References

Allen, A. J., Thomas, J. J. and Jennings, H. M. (2007). Composition and density of nanoscale calcium-silicate-hydrate in cement. *Nature Materials*, *6*(4), 311-316. https://doi.org/Doi 10.1038/Nmat1871

Auroy, M., Poyet, S., Le Bescop, P., Torrenti, J.-M., Charpentier, T., Moskura, M. and Bourbon, X. (2018). Comparison between natural and accelerated carbonation (3% CO2): Impact on mineralogy, microstructure, water retention and cracking. *Cement and Concrete Research*, *109*, 64-80. https://doi.org/https://doi.org/10.1016/j.cemconres.2018.04.012

Bary, B. and Sellier, A. (2004). Coupled moisture-carbon dioxide-calcium transfer model for carbonation of concrete. *Cement and Concrete Research*, *34*(10), 1859-1872. https://doi.org/DOI 10.1016/j.cemconres.20004.01.025

Berner, U. R. (1992). Evolution of pore water chemistry during degradation of cement in a radioactive waste repository environment. *Waste Management*, *12*(2–3), 201-219. https://doi.org/10.1016/0956-053x(92)90049-o

Morandeau, A., Thiéry, M. and Dangla, P. (2014). Investigation of the carbonation mechanism of CH and C-S-H in terms of kinetics, microstructure changes and moisture properties. *Cement and Concrete Research*, *56*(0), 153-170. https://doi.org/http://dx.doi.org/10.1016/j.cemconres.2013.11.015

Muntean, A., Bohm, M. and Kropp, J. (2011). Moving carbonation fronts in concrete: A moving-sharp-interface approach. *Chemical Engineering Science*, *66*(3), 538-547. https://doi.org/DOI 10.1016/j.ces.2010.11.011

Papadakis, V. G., Vayenas, C. G. and Fardis, M. N. (1991). Experimental Investigation and Mathematical-Modeling of the Concrete Carbonation Problem. *Chemical Engineering Science*, *46*(5-6), 1333-1338.

Phung, Q. T. (2015). *Effects of Carbonation and Calcium Leaching on Microstructure and Transport Properties of Cement Pastes* [PhD thesis, Ghent University]. Belgium.

Phung, Q. T., Maes, N., Jacops, E., Jacques, D., De Schutter, G. and Ye, G. (2019a). Insights and issues on the correlation between diffusion and microstructure of saturated cement pastes. *Cement and Concrete Composites*, *96*, 106-117. https://doi.org/https://doi.org/10.1016/j.cemconcomp.2018.11.018

Phung, Q. T., Maes, N., Jacques, D., Bruneel, E., Van Driessche, I., Ye, G. and De Schutter, G. (2015). Effect of limestone fillers on microstructure and permeability due to carbonation of cement pastes under controlled CO2 pressure conditions. *Construction and Building Materials*, *82*(0), 376-390. https://doi.org/http://dx.doi.org/10.1016/j.conbuildmat.2015.02.093

Phung, Q. T., Maes, N., Jacques, D., De Schutter, G., Ye, G. and Perko, J. (2016a). Modelling the carbonation of cement pastes under a CO2 pressure gradient considering both diffusive and convective transport. *Construction and Building Materials*, *114*, 333-351. https://doi.org/http://dx.doi.org/10.1016/j.conbuildmat.2016.03.191

Phung, Q. T., Maes, N., Jacques, D., Schutter, G. d. and Ye, G. (2016b). Effect of Limestone Fillers on Ca-Leaching and Carbonation of Cement Pastes. *Key Engineering Materials*, *711*, 269-276. https://doi.org/10.4028/www.scientific.net/KEM.711.269

Phung, Q. T., Maes, N. and Seetharam, S. (2019b). Pitfalls in the use and interpretation of TGA and MIP techniques for Ca-leached cementitious materials. *Materials & Design*, *182*, 108041. https://doi.org/https://doi.org/10.1016/j.matdes.2019.108041

Varzina, A., Phung, Q. T., Perko, J., Jacques, D., Maes, N. and Cizer, Ö. (In preparation). Carbonation of fractured cement paste – synergistic effects of w/c ratio, relative humidity and CO2 concentration on microstructural and mineralogical alteration. *Cement & Concrete Composites*.